AD-A136 266 CHARACTERISTICS OF GAMMA-RAY LINE FLARES(U) STANFORD 1/1
UNIV CA INST FOR PLASMA RESEARCH T BAI ET AL. OCT 83
SU-IPR-961 N00014-75-C-0673

UNCLASSIFIED F/G 3/2 NL

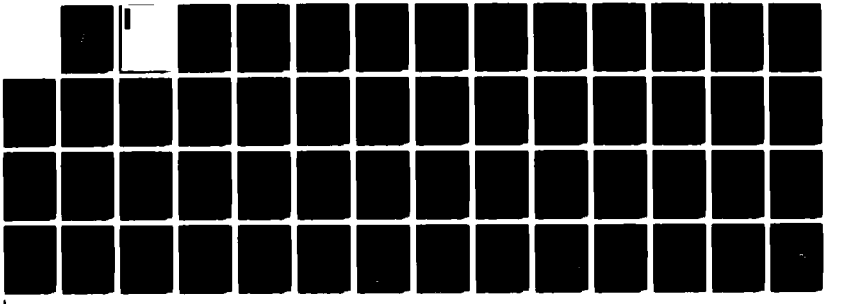

END
DATE FILMED
2-84
DTIC

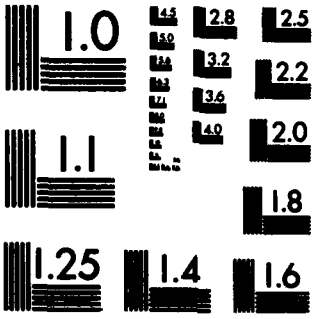

MICROCOPY RESOLUTION TEST CHART
NATIONAL BUREAU OF STANDARDS-1963-A

CHARACTERISTICS OF GAMMA-RAY LINE FLARES

Taeil Bai
Stanford University
Stanford, CA 94305

and

Brian Dennis
Goddard Space Flight Center
Greenbelt, MD 20771

ABSTRACT

Observations of solar gamma rays by the Solar Maximum Mission (SMM) have demonstrated that energetic protons and ions are rapidly accelerated during the impulsive phase. In order to understand the acceleration mechanisms for these particles, we have studied the characteristics of the gamma-ray line flares observed by SMM. Because we discovered that the gamma-ray line flares emit very intense hard X-rays, we have also studied very intense hard X-ray flares without detectable gamma-ray lines. The following characteristics distinguish gamma-ray line flares from other flares:

(1) Intense hard X-ray and microwave emissions;

(2) Delay of high-energy hard X-rays;

(3) Emission of type II and/or type IV radio bursts; and

(4) Flat hard X-ray spectra (average power-law index: 3.1).

cont'd from

The majority of the gamma-ray line flares shared all these characteristics, and the remainder shared at least three of them. Among gamma-ray line flares we have found positive correlations between the following pairs of quantities: (a) durations of spike bursts and spatial sizes of flare loops; and (b) delay times and durations of spike bursts.

CHARACTERISTICS OF GAMMA-RAY LINE FLARES

I. INTRODUCTION

Energetic protons and heavy ions accelerated in solar flares produce gamma rays by interacting in the solar atmosphere (Lingenfelter and Ramaty 1967; Ramaty, Kozlovsky, and Lingenfelter 1975). Therefore, by observing solar gamma rays, we can obtain information on the acceleration and interaction of these particles. The Gamma Ray Spectrometer (GRS) was installed on the Solar Maximum Mission (SMM) to do just that. Until late 1981 SMM observed gamma-ray lines from more than ten flares (Rieger 1982), and observed several more gamma-ray line flares during the first half of 1982 (Share et al. 1982), exceeding modest pre-launch expectations.

One of the important results emerging from these observations is that protons and heavy ions are rapidly accelerated during the impulsive phase (Forrest et al. 1981; Chupp 1982; Chupp et al. 1982). It was known from earlier observations (Chupp et al. 1973; Hudson et al. 1980; Prince et al. 1982) that protons and heavy ions are accelerated during the impulsive phase, but the rapidity of acceleration is a discovery made by SMM. At least in some flares, the characteristic time

for ion acceleration seems to be as short as a few seconds (e.g., Forrest et al. 1981; Chupp et al. 1982).

Until recently, it was widely accepted that protons and heavy ions as well as relativistic electrons are accelerated during the second phase of a flare, which is manifested by type II and IV radio bursts observed several minutes after the impulsive phase (Wild, Smerd, and Weiss 1963; de Jager 1969; Svestka 1976; Bai and Ramaty 1976). This view was gleaned from the association of energetic protons observed in the interplanetary medium with type II and IV radio bursts. However, recent observations of solar gamma rays make the conventional view no longer tenable, requiring developments of new ideas and interpretations (Chupp 1982; Bai 1982).

The purpose of this paper is to show that gamma-ray line flares, as a group, possess characteristics that set them apart from non-gamma-ray line flares. Such a study, using the large number of gamma-ray line flares now identified, can yield valuable insight that is not obtainable from studying the few gamma-ray line flares observed before the launch of SMM. The emphasis of the study was on hard X-ray emissions, because from them we can obtain information on nonthermal electrons, which are believed to carry a large fraction of the total flare

energy. First of all, we studied the hard X-ray fluxes observed by the Hard X-Ray Burst Spectrometer (HXRBS; cf., Orwig, Dennis, and Frost 1980) and found that the gamma-ray line flares are very intense hard X-ray flares. For comparison, we also studied the 14 most intense hard X-ray flares observed during 1980 with HXRBS that did not emit observable gamma-ray lines. We studied the general morphology of hard X-ray time profiles, and we searched for delays of the high-energy hard X-rays, which are interpreted as an indication of "second-step" acceleration (Bai and Ramaty 1979; Bai 1982; Bai et al. 1983b). In addition to hard X-rays, we studied type II and IV radio bursts, and microwave and H α emissions associated with the flares.

II. CHARACTERISTICS OF GAMMA-RAY LINE FLARES

A. Gamma-Ray Line Flares and Hard X-ray Fluxes

The characteristics of all gamma-ray line flares used in this study are given in Table 1. All of these flares were observed with GRS and HXRBS on SMM during 1980 and 1981. Some of these flares have been discussed in the literature (e.g., Forrest et al. 1981; Chupp 1982, 1983; Chupp et al. 1982, 1983). A complete list of gamma-ray line flares observed by SMM until the end of 1981 is given in Figure 3 of Rieger (1982). In

addition to the ten gamma-ray line flares identified by Rieger, we add to the list two more flares that occurred on 1981 October 7 and 14. Hinotori detected gamma-ray lines from both flares (Yoshimori et al. 1983), and the 1981 October 7 flare was later identified as a gamma-ray line flare by the GRS group (Share et al. 1982). We think that GRS did not detect a significant flux of 2.2-MeV line photons from the October 14 flare because it was a limb flare and because SMM was eclipsed after observing only the first 80 s of the impulsive phase.

We have not included in this list of gamma-ray line flares those flares that showed no resolved gamma-ray line emission but did show an excess counting rate in the 4 - 7 MeV, even though this excess has been interpreted to be of nuclear origin (see Chupp 1982; Ramaty et al. 1982). The reason for omitting these flares is as follows: Protons and heavy ions with relatively low energy (4 ~ 10 MeV/nucleon) can produce gamma-ray lines in the 4 - 7 MeV range; but in order to produce the 2.2 MeV line, higher-energy (several tens of MeV/nucleon) particles are necessary (Ramaty, Kozlovsky, and Lingenfelter 1975). Therefore, detection of the 2.2 MeV line is a sure indication that a large number of protons and ions are accelerated to enegies > 10 MeV/nucleon.

The hard X-ray characteristics of the gamma-ray line flares were determined from the HXRBS observations. First, we determined the peak hard X-ray counting rates measured by HXRBS, using the HXRBS event listing (Dennis et al. 1983). We found that all the gamma-ray line flares produced hard X-ray emissions with HXRBS peak count rates > 7500 counts s^{-1} (all but two flares were > 10^4 counts s^{-1}). Figure 1 shows the number of hard X-ray events observed during 1980 and 1981 versus the HXRBS peak rate. The shaded portion indicates the number of these flares that are also gamma-ray line flares. As can be seen, intense hard X-ray flares are likely to be gamma-ray line flares. Conversely, gamma-ray line flares are generally intense hard X-ray flares. Therefore, if we study only the gamma-ray line flares, unwittingly we may end up finding the characteristics of very intense hard X-ray flares--the so-called "big flare syndrome" (Kahler 1982a). Thus, it is necessary also to study non-gamma-ray line flares with peak HXRBS rates > 10^4 counts/s. During 1980, 14 such flares were detected. We chose to use these 14 flares as a comparison group, and their characteristics are given in Table 2.

B. Hard X-ray Time Profiles

The first two flares from which gamma-ray lines were detected (Chupp et al. 1973) occurred on 1972 August 4 and 7. The hard X-ray emission from these flares lasted more than 10 minutes, and such flares were dubbed extended-burst flares (Hoyng, Brown, and van Beek 1976). The H α classifications of these flares are 3B. The next well-observed gamma-ray line flare was also an extended hard X-ray burst and a 2B flare (Hudson et al. 1980). From such observations, it was inferred that gamma-ray lines are more likely to be produced in flares which are extended both temporally and spatially. The first gamma-ray line flares observed by SMM ran counter to this notion, and this fact has been well publicized (Chupp 1982; Forrest et al. 1981). Because we investigate 12 gamma-ray line flares in this paper, we can determine whether there are general properties in the hard X-ray time profiles of these flares.

Figure 2 shows the hard X-ray time profiles of the gamma-ray line flares, plotted with the same time scale. We chose the X-rays in channels 6 - 8 of HXRBS, corresponding to an energy range that varied from 114 - 183 keV in February 1980 to 140 - 226 keV in December 1981 (Dennis et al. 1983). We chose these channels because in the lower energy channels contributions from

a slowly varying component are substantial. This low-energy component is interpreted to be thermal radiation by a very hot ($> 2 \times 10^7$ K) plasma (Bai and Orwig 1983). In Figure 2 we arranged the time profiles roughly in order of impulsiveness instead of in chronological order. In the most impulsive events, the durations of individual bursts are less than 10 s. On the other hand, in the least impulsive events, the burst durations are longer than 2 minutes. In the extreme case of the 1981 April 26 flare, one gradual burst lasted more than 10 minutes. By analyzing the gamma-ray line flares observed by Hinotori, Yoshimori et al. (1983) concluded that there are two classes of gamma-ray line flares—impulsive and gradual. However, we get a different impression from Figure 2. Although the durations of the spikes span two orders of magnitude, they seem to be quite evenly distributed, instead of being clustered around preferred values.

C. The Delay of High-Energy Hard X-Rays in Gamma-Ray Line Flares

Bai et al. (1983b) emphasized the fact that the delays of high-energy hard X-rays had all been observed from gamma-ray line flares or proton flares. From this fact these authors proposed that a second-step mechanism accelerates both gamma-ray producing protons and mildly relativistic electrons. Therefore,

we searched for delays of high-energy hard X-rays. We visually inspected the computer-generated time profiles of different energy bands by superposing them. This method turns out to be very efficient and effective, because we can easily look at the time profiles in arbitrary detail down to the detector resolution 0.128 s. It was our practice to study the time profiles of the following five energy bands: band 1 (ch. 1 - 2: 30 - 59 keV), band 2 (ch. 3 - 5: 59 - 135 keV), band 3 (ch.6 - 8: 135 - 218 keV), band 4 (ch. 9 - 11: 218 - 310 keV), band 5 (ch. 12 - 15: 310 - 521 keV). We found delays of high energy hard X-rays from most of the gamma-ray line flares. The delay time usually increases with X-ray energy. In most of the gamma-ray line flares, the time profile of band 1 is dominated by the slowly-varying thermal component (cf. Figs. 3 and 4); therefore, in these cases the delay is estimated with respect to the time profile of band 2. For some cases when the time profile of band 2 is also dominated by the low-energy component, the delay is estimated with respect to the time profile of band 3. The delay discussed below is that of the band 5 time profile with respect to that of band 2, unless otherwise indicated.

Examples of delays are shown in Figures 5 - 7. Figure 5 shows the time profiles of the first of the three bursts of the

1981 February 26 flare. A delay of ~ 1 s can be seen here for the 216 - 309 keV X-rays. Figure 6 shows an example of intermediate-range delays. The delay of the 218 - 311 keV X-rays is about 6 s. Figure 7 shows the time profiles of the 1981 April 26 flare, from which the longest delay is found. We can find from these figures that the delays are due to the shifts of the whole time profiles along the time axis. The high-energy time profiles start somewhat later, peak later, and decay later than the low-energy time profiles. In spectral evolution, this trend shows up as flattening of the hard X-ray spectrum with time throughout individual bursts.

In addition to visual inspections, we also estimated the delays by calculating cross-correlation functions for some flares. The results are given in Table 3. The delays estimated from visual inspections are in agreement with these results to within 30 percent. Except for the 1981 April 26 flare, we calculated cross-correlation functions with respect to the time profiles of channels 3 - 5 because of the dominant contribution from the slowly varying component to the flux in channels 1 - 2. In the following we discuss the results of our search for delays, flare by flare in order of appearance in Figure 2.

(1) 1980 June 7 flare

This is the most spiky (impulsive) event, with spike durations of less than 10 seconds. There was no apparent delay of high-energy hard X-rays. However, interestingly, the 4 - 6 MeV gamma-ray time profile exhibits a 2-s delay (Chupp 1982; Bai 1982). Also, the 17 GHz microwave time profile shows about a 1-s delay with respect to the hard X-ray time profiles (Kane et al. 1983). Because the 17 GHz microwaves are mainly produced by relativistic electrons (Bai and Ramaty 1976), the delay of the microwaves indicates that the relativistic electrons were probably delayed in this flare. Kiplinger et al. (1983) have suggested that the 2-s delay of the 4 - 7 MeV gamma rays may result from a second, harder peak appearing in each individual burst.

(2) 1980 July 1 flare

This is also a very spiky event. There was no apparent delay in the main feature of the flare, but we found delays in the spike bursts that occurred during the decay phase of the flare. For the burst centered around 1627:55 UT, the time profile of band 4 (134 - 216 keV) showed a 1.3-s delay; for the burst centered around 1628:25 UT, a 3.8-s delay. The time profile of band 5 is too noisy to estimate the delay.

(3) 1981 February 26 flare

The time profiles for this event consist of three conspicuous spike bursts. For the first spike, the time profile of band 4 is delayed by 0.8 s with respect to that of band 2 (Fig. 4). The time profile of band 5 is too noisy. There is no apparent delay for the second and third spikes.

(4) 1980 June 21 flare

No apparent delay of high-energy hard X-rays is found from this flare. However, the 35 GHz microwave time profile is delayed by ~ 2 s with respect to the hard X-ray time profiles (Nakajima, Kosugi, and Kai 1982). Also, the time profile of the gamma-ray continuum above 10 MeV, which is probably due to bremsstrahlung of relativistic electrons (Ramaty et al. 1983), is delayed by about 5 s (Rieger 1982).

(5) 1981 September 7 flare

The time profile consists of one main burst (2223 - 2223:40 UT), with several less intense bursts following it. In the main burst, the delay is not obvious upon visual inspection because the time profiles of high-energy channels are quite noisy. Calculating the correlation functions, however, we find a delay that increases with energy. The delay for channels 12 - 15

(349 - 528 keV) is ~ 1.5 s. The hard X-ray spectrum flattened monotonically during the main burst in a manner consistent with such a delay.

(6) 1980 November 6 flare

This event consists of two major spikes. For the first spike we found a 1-s delay; for the second spike, a 2-s delay. These delays were obtained by comparing the time profile of band 3 with that of band 5. Delays calculated from cross-correlating are given in Table 3.

(7) 1981 October 14 flare

This event consists of two spikes, a small spike followed by a large one. For the large spike, the time profile of band 5 is delayed by 3.5 s with respect to that of band 2. For the small spike, we could confirm a delay of a few seconds, but we could not estimate the delay accurately because of the proximity of the large spike burst.

(8) 1981 April 1 flare

This event consists of three intervals of hard X-ray emission. In the first interval there are two spike bursts, and the delay for this interval is ~ 5 s. In the second interval

there is one major burst, with minor ones preceding and following it. In the major burst we found a 5-s delay. In the first burst (peaking at 0150:30 UT) of the third interval, we found a 5-s delay. In the main burst of the third interval, we found an 8-s delay.

(9) 1981 October 7 flare

This was a limb flare. There are three spike bursts in the time interval between 2255:40 UT and 2257:40 UT (Fig. 3). The delay time for these three spikes is about 5 s. The delay for the two small spike bursts peaking at about 2258:00 UT and 2258:30 UT is about 2 s. The time profile after 2259 UT consists of three or four spike bursts. The first two of these are easily seen in Figure 2; the delay time for them is about 10 s. The remaining two spike bursts (centered around 2301:10 UT and 2301:30 UT) are seen in the time profiles of lower energy bands but are not obvious in the time profile shown in Figure 2. For this very reason, the delay for these bursts could not be estimated visually. The delays averaged over the entire impulsive phase are given in Table 3.

(10) 1981 April 10 flare

This time profile can be divided into two prominent structures. It is difficult to estimate visually the delay times for the first structure, because it consists of 4 to 5 spike bursts, the relative strengths of which change with energy. The second structure is dominated by a spike burst peaking at 1651:10 UT, and the delay time for this burst is about 10 s (Fig. 6).

(11) 1981 April 27 flare

Hard X-ray (10 - 36 keV) imaging of this limb event by Hinotori (Tsuneta et al. 1982) shows that the source is located 12,000 km above the limb. As far as the hard X-ray time profile is concerned, this flare is quite similar to the gamma-ray line flares of 1972 August 4 and 7. However, unlike the latter flares, it produced neither a strong interplanetary shock nor a high flux of interplanetary protons. This extended burst consists of many spike bursts, some of which are close to each other and some of which are well separated in time. For the structure between 0806:30 UT and 0809:50 UT, no delay is found. For the structure between 0810 UT and 0812 UT, it is about 7 s. Between 0812 and 0814:40 UT, it is 10 s; between 0816:30 and 0819 UT, 3 s.

(12) 1981 April 26 flare

This flare occurred in the same active region as the April 27 flare. This flare is unusual in several respects. First, the hard X-ray emission of this flare is one of the longest in duration. The hard X-ray emission started at ~ 1100 UT and lasted until 1155 UT, when SMM went into the Earth's shadow. Second, the impulsiveness of the hard X-ray emission varied with time. The hard X-ray emission time profile is quite spiky until 1133 UT, after which it is very gradual. Only the latter part, during which gamma rays were observed, is shown in Figures 2 and 7. Third, the delay time is the longest: The delay of the 311 - 511 keV hard X-rays with respect to the 30 - 59 keV hard X-rays is as large as 2 min (cf. Fig. 7 and Table 3). Fourth, the microwave emission was extremely intense (10,000 sfu at 9 GHz); and when normalized with respect to the hard X-ray flux, it is the largest among the flares studied in this paper. Such long-duration, gradual hard X-ray bursts are rarely observed, and all of them (occurring on 1969 March 30, 1971 December 14, and 1972 July 22) were high coronal sources (~ 20,000 km), judging from the limb occultation (Frost and Dennis 1971; Hudson 1978b; Hudson, Lin, and Stewart 1982). From this we can infer that the

hard X-ray emission of this flare probably emanated from the high corona. We plan to study this flare in further detail.

D. The Delay of High-Energy Hard X-Rays in Non-Gamma-Ray Line Flares

We searched for delay of high-energy hard X-rays from the non-gamma-ray line flares in a manner similar to that described above. Among the 14 non-gamma-ray line flares that we have studied, we found high-energy hard X-ray delays from only two flares, which occurred on 1980 May 21 and July 21--about 1-s delay for the former and about 2-s delay for the latter.

E. Hard X-Ray Spectra

It is well known that the hard X-ray spectrum is not constant but changes with time during a typical flare (e.g., Kane and Anderson 1970; Hoyng et al. 1976). Large changes of spectral shape usually occur during the very early part of the impulsive phase or during the decay part, and during the rest of time the hard X-ray spectral shape changes relatively little. In order to see whether the hard X-ray spectra of gamma-ray line flares are different from the spectra of non-gamma-ray flares, we did the following: First, for each flare we took one interval around the maximum of the time profile of energy band 3 (135 -

218 keV). Second, we accumulated X-ray counts for this interval and fitted the results with a power-law photon-energy spectrum, deleting channels 1, 2, and 15. As we mentioned earlier, for many flares the hard X-ray counts of the first two channels are dominated by contributions from a very hot thermal component (see Lin et al. 1981; Bai and Orwig 1983), and the width of channel 15 is not well known. For most cases a single power-law spectrum provides good fits to the data, although in some cases exponential spectra provide better fits (e.g., Dennis et al. 1981; Kiplinger et al. 1983). The resultant spectral indices are presented in Tables 1 and 2. In obtaining these spectra, we made pulse pileup corrections, which are important when the counting rates exceed $1 \sim 3 \times 10^4$ counts s^{-1} (Datlowe 1975, 1977).

Comparing the spectral indices given in Tables 1 and 2, we find that the hard X-ray spectra of gamma-ray line flares are on the average flatter than those of non-gamma-ray line flares. The average spectral index of the gamma-ray line flares is 3.2, and the standard deviation is 0.5. The average spectral index of the non-gamma-ray line flares is 4.3, and the standard deviation is 0.7. The average spectral indices of these two populations are separated by about the sum of the standard

deviations, which means that the separation is statistically significant. The spectral indices given here are generally somewhat smaller than those given in the earlier paper (Bai et al. 1983a) because in the earlier work we did not delete channels 1 and 2 for spectral fits.

F. Radio Bursts, H α Classes, and Other Phenomena

Originally, good associations of type II and IV radio bursts with proton flares led to the idea that protons are accelerated during the second phase of flares (Wild, Smerd, and Weiss 1963; de Jager 1969; Svestka 1976). Although we now know that nuclear gamma rays are observed during the impulsive phase, we searched for type II and IV radio bursts associated with the flares studied in this paper, using the Solar Geophysical Data. The results are tabulated in Tables 1 and 2. We see a sharp contrast between gamma-ray line flares and non-gamma-ray line flares. All but two flares produced type II radio bursts, and all but three flares produced type IV radio bursts. On the other hand, only three of the non-gamma-ray line flares are associated with type II and IV radio bursts.

H α classifications of the flares are also given in the tables. The Hα classes of the gamma-ray line flares range from importance S to 3, but we do not see any obvious difference

between the two groups of flares. Subflares were not expected to produce gamma-ray lines.

The microwave flux densities measured at ~ 9 GHz are also given in the tables. We find here that all the gamma-ray line flares produced very intense microwaves.

The hard X-ray start time is defined as the time when the flux of energy band 3 (135 - 220 keV) becomes 10 percent of the maximum flux for the first time. The hard X-ray end time is defined similarly. The duration of hard X-ray emission, which is denoted as D in Tables 1 and 2, is the interval between the hard X-ray start time and the end time. This duration is, in general, considerably smaller than the duration given in Dennis et al. (1983). The durations given in Tables 1 and 2 cover a range of more than an order of magnitude, but we cannot find any clear trend separating the gamma-ray line flares from the other flares.

III. SUMMARY AND DISCUSSION

A. Summary

The characteristics of the gamma-ray line flares discussed in the preceding section are summarized below.

(1) **Very intense hard X-ray emissions**: Except for two gamma-ray line flares, the peak fluxes observed by HXRBS exceed 10^4 counts s^{-1}. Of about 4,300 solar flares detected with HXRBS through the end of 1981, only 40 flares had peak rates > 10^4 counts s^{-1}.

(2) **Delay of high-energy hard X-rays**: Delays are found from most gamma-ray line flares.

(3) **Type II and IV radio bursts**: Such radio bursts are observed from most gamma-ray lines flares.

(4) **Flat hard X-ray spectra**: The hard X-ray spectra of the gamma-ray line flares are on the average flatter than those of the non-gamma-ray line flares.

(5) **Very intense microwave emissions**: For all the gamma-ray line flares, the peak flux density at 9 GHz is > 500 sfu. (For all but two, it is > 1000 sfu.)

These are the characteristics that distinguish gamma-ray line flares from the others. Most gamma-ray line flares exhibit all of the above-mentioned characteristics, and all of them exhibit at least three. The non-gamma ray line flares we have

chosen to study in this paper are all very intense hard X-ray flares (HXRBS peak rate > 10^4 counts s^{-1}). By selection, they all share the first-mentioned characteristic, but generally they do not exhibit many of the other characteristics. Among the non-gamma-ray line flares, only the 1980 May 21 flare exhibits all the characteristics of gamma-ray line flares. Considering that its hard X-ray flux is relatively low and its duration is short (cf. Table 2), this flare could have been a weak gamma-ray line flare.

H α importance of gamma-ray line flares ranges from S to 3, and from H α data only there is no way of distinguishing gamma-ray line flares from others. However, when we use the Hα importance as an indication of the size of the flare loop, we find an interesting point. There seems to be a correlation between the duration of spike bursts and the spatial size of the flare. The flares near the top of Table 1 (flares with short-duration spike bursts) are of H α importance class S or 1, indicating small flare loops. The flares near the bottom of Table 1 are of H α class 2 or 3, except the limb flare of 1981 October 7, for which the H α importance is not a good indication of flare size. For this limb flare as well as another limb flare of 1981 April 27, Hinotori imaging results show that hard

X-ray (17 - 40 keV) emissions come from high (> 10,000 km) in the corona. The 1981 April 26 flare is of only Hα importance 2, but this flare shows all the characteristics of very high coronal X-ray sources—gradual rise and fall of hard X-ray flux, long duration, and no rapid variation of hard X-ray flux (see, Frost and Dennis 1971; Hudson 1978; Hudson, Lin, and Stewart 1982; Bai 1982). Therefore, we can see a trend: the size of the flare loop increases as we move downward in Table 1.

There seems to be a correlation between the delay time and the duration of spike bursts of each flare. In Table 1 the flares are arranged roughly in order of decreasing impulsiveness—flares with the most spiky time profiles at the top and the ones with the longest bursts at the bottom. As we can see, the flares near the top show no apparent delay or only short delays, and the delay time shows a trend of increase toward the bottom.

B. Discussion

First of all, the fact that gamma-ray line flares, as a group, possess a distinct set of characteristics suggests that gamma-ray producing protons are not abundantly accelerated in all flares. If all flares produce gamma-ray lines and only the GRS detector threshold effect distinguishes the gamma-ray line

flares from the rest, we do not expect the gamma-ray line flares to exhibit distinct characteristics. All the flares studied in this paper (see Tables 1 and 2) have peak HXRBS count rates greater than 7500 ct s^{-1}. But this hard X-ray flux threshold did not make these flares, as a group, possess distinct characteristics. Only when we separate the gamma-ray line flares do they exhibit a distinct set of characteristics. Therefore, we can conclude that only in a small fraction of flares does a mechanism (or mechanisms) accelerate protons to gamma-ray producing energies. We can learn more about this mechanism by expanding on the above-mentioned characteristics, point by point.

First, the intense hard X-ray fluxes of the gamma-ray line flares are probably due to the following two threshold effects—the GRS threshold for detection of lines and a threshold flare energy for proton acceleration. If there is some correlation between the hard X-ray flux and the gamma-ray line flux—the big flare syndrome (Kahler 1982a), flares producing detectable gamma-ray line fluxes are more likely to produce intense hard X-ray emissions. If proton acceleration is a secondary result of the large amount of energy release (see Lin and Hudson 1976; Hudson 1978a), gamma-ray lines are to be observed only from

flares with large energy release. The fact that the gamma-ray line flares show a set of distinct characteristics indicates that the detector threshold effect is not the sole cause of the intense hard X-ray fluxes of the gamma-ray line flares.

Second, the delay of hard X-rays is an indication that a second-step mechanism accelerates (mildly) relativistic electrons (Bai and Ramaty 1979). The fact that the hard X-ray delays are predominantly found from gamma-ray line flares suggests that the second-step mechanism also accelerates protons. Note here that the gamma-ray time profiles are in general also delayed with respect to the low-energy hard X-ray time profiles (Gardener et al. 1981; Rieger 1982; Yoshimori et al. 1983). One can explain the hard X-ray delays with a trap model (Bai and Ramaty 1979; Vilmer et al. 1982), but the trap model is not compatible with other observations (Bai, Kiplinger, and Dennis 1983; Bai and Orwig 1983). In the trap model, the bulk of the energy of nonthermal electrons is originally deposited in a trap region with densities of order of few times 10^{10} cm^{-3}, but various SMM observations indicate the bulk of the energy is deposited in the chromosphere (Hoyng et al. 1981; Antonucci et al. 1982; Acton et al. 1982).

Third, the association of type II and IV radio bursts with the gamma-ray line flares is very interesting. Type II and IV radio bursts are believed to be produced during the second phase by shocks in the high corona. By extrapolating the propagation of type II shocks backward in time, one can infer that these shocks originate during the impulsive phase at the flare site (e.g., Wild, Smerd, and Weiss 1963; Maxwell and Dryer 1981). The finding that type II and IV radio bursts occurring in the high corona are associated with the phenomena taking place during the impulsive phase (gamma-ray production and high energy hard X-ray delay) is much stronger evidence that type II shocks originate during the impulsive phase. But it is still not well understood how and when progenitors of type II shocks are produced. It is also not well understood whether the progenitor is a shock in the flare loop or a disturbance that later develops into a shock in the corona. If it is a shock in the flare loop, we do not know how it escapes instead of being confined in the loop. But because MHD shocks are known to be good accelerators, it is tempting to say that type II shocks start as shocks in the flare loop. Bai et al. (1983b) proposed as a second-step mechanism a first-order Fermi process by shocks propagating in the flare loop.

Fourth, the flatter hard X-ray spectra of gamma-ray line flares may be due to either of two effects. First, the electron spectrum (consequently, the hard X-ray spectrum) becomes flatter for the gamma-ray line flares because of the second-step acceleration. Second, flatter hard X-ray spectra indicate that the primary (first-step) mechanism accelerated a relatively larger number of high energy electrons and also a larger number of high-energy protons. Therefore, for flares with flatter hard X-ray spectra larger numbers of protons are injected for the second-step acceleration. The fact that flares with no second-step hard X-ray delays (such as the ones on 1980 June 7 and 21) have flat spectra favors the second possibility.

Fifth, the apparent correlation between the flare loop lengths and the duration of spike bursts can be explained by the following scenario. If energy is stored over the volume of the entire flare loop and is released in a localized region, the energy release time (spike burst duration) is likely to be correlated with the size of the loop (e.g., Sturrock 1980).

Sixth, we can speculate that the correlation between the delay times and the loop size is due to the following scenarios. According to Bai _et al._ (1983b), the characteristic time for the second-step acceleration is the transit time of a shock through

the flare loop. In this model, it is necessary to scatter pitch angles of energetic electrons in order for the second-step mechanism to accelerate efficiently; therefore, if the loop length is smaller than the mean free path for pitch angle scattering for electrons, the second-step mechanism would not work for energetic electrons. In this view, for the gamma-ray line flares thought to have short loops (the ones near the top of Table 1), the loop lengths are shorter than the mean free path for electron scattering but longer than those for energetic protons.

Is there a need for a second-step acceleration, in addition to the observations discussed in this paper? The answer is yes. First, the energy spectrum of protons and that of electrons of a given flare are drastically different. At low energies ($\lesssim$ 300 keV), energetic electrons are much more numerous than energetic protons (cf. Canfield et al. 1980); on the other hand, at high energies (> 1 MeV) energetic protons are much more numerous than energetic electrons (Ramaty et al. 1980, 1983). This is very difficult to explain with a single acceleration mechanism. Second, it is well known that certain acceleration mechanisms are efficient for particles above threshold energies, which are often called "injection energies." Such is the case for Fermi-

type accelerations (Ginzburg and Syrovatskii 1964) and for the stochastic acceleration proposed by Sturrock (1974). On the other hand, a dc electric field or a low-frequency electric field can promptly accelerate particles to low energies, but the maximum energy is limited by the potential drop. It is hard to imagine the existence of a potential drop much larger than 1 MeV in solar flare sites. For these reasons Bai (1982) proposed, before analyzing the SMM gamma-ray line flares in detail, that a second-step acceleration is responsible for both gamma-ray producing protons and (mildly) relativistic electrons

It is appropriate to discuss here the recent work on proton flares (Kahler 1982b; Cliver, Kahler, and McIntosh 1983). Kahler (1982b) discusses the evidence that not all the type II events that occurred in magnetically well-connected regions are associated with proton flares. We can make an analogous conclusion: not all the type II events are associated with gamma-ray line flares. Type II events occur much more frequently than gamma-ray line flares or proton flares. In terms of Hα classifications, there seems to be a slight difference between gamma-ray line flares and proton flares. Less than 10 percent of the proton flares (4 of 52) are sub-flares (S class), whereas one-third of the gamma-ray line flares

(4 of 12) are sub-flares. Because the sample numbers are small, we cannot draw a strong conclusion from this; nevertheless, this difference should be studied in the future. The big difference between the proton flares and the gamma-ray line flares, however, is in the strength of the impulsive phase. All the gamma-ray line flares have a very intense impulsive phase: their peak HXRBS rates are the highest (> 7,500 counts/s) and their peak flux densities at about 9 GHz are greater than 500 sfu (mostly > 1000 sfu). On the other hand, many proton flares show weak impulsive phases: of the 46 proton flares, 17 flares produced 9 GHz microwaves with peak flux density of less than 1000 sfu, and 8 flares less than 100 sfu (Cliver, Kahler, and McIntosh 1983). In addition to these, even for gamma-ray line flares occurring in magnetically well-connected regions, there seems to be little correlation between the gamma-ray line intensity and the interplanetary proton flux (e.g., von Rosenvinge, Ramaty, and Reames 1981; Pesses et al. 1981; Yoshimori et al. 1983). These differences between gamma-ray line flares and proton flares may be due to different acceleration mechanisms or may simply be due to different magnetic field configurations. If some magnetic field lines in the acceleration region are connected to the interplanetary

medium, accelerated protons and relativistic electrons are more likely to escape, making gamma-ray production and microwave emission less efficient.

As mentioned in the introduction, the flares which produced excess gamma rays in the 4 ~ 7 MeV region but did not produce a significant flux (> 2 sigma) of 2.2-MeV line photons have not been regarded as gamma-ray line flares in this study. Three of the flares in Table 2 are such flares. The inclusion of them in Table 1 will not change the conclusions of this paper, although they do not seem to share the important characteristics of gamma-ray line flares.

In conclusion, the fact that gamma-ray line flares exhibit characteristics that distinguish them from other flares means that the acceleration mechanism for protons and heavy ions with energy > 10 MeV/nucleon is different from the primary acceleration. The fact that delay of high-energy hard X-rays is mainly observed from gamma-ray line flares indicates that the same mechanism (or mechanisms of the same origin) accelerates both mildly relativistic electrons and gamma-ray producing protons. This mechanism, which is called the second-step mechanism (Bai and Ramaty 1979; Bai 1982; Bai et al. 1983b), is

still not claimed to be known, although several candidates have been proposed.

During this research Bai was supported by NASA grants NGL 05-020-272 and NAGW-92 and ONR contract N00014-75-C-0673 at Stanford University and by NASA grant NSG-7161 at UCSD. Bai thanks Ken Frost for his hospitality. We thank Alan Kiplinger, Larry Orwig, Harold Dennis, and Shelby Kennard for assistance in analyzing the HXRBS data.

REFERENCES

Acton, L. W., Canfield, R. C., Gunkler, T. A., Hudson, H. S., Kiplinger, A. L., and Leibacher, J. W. 1982, Ap. J., 263, 409.

Antonucci, E. et al. 1982, Solar Phys., 78, 107.

Bai, T. 1982, in Gamma Ray Transients and Related Astrophysical Phenomena, R. E. Lingenfelter (ed.), (New York: American Inst. of Physics), p. 409.

Bai, T., Dennis, B. R., Kiplinger, A. L., Orwig, L. E., and Frost, K. J. 1983a, Solar Phys. (in press).

Bai, T., Hudson, H. S., Pelling, R. M., Lin, R. P., Schwartz, R. A., and von Rosenvinge, T. T. 1983b, Ap. J., 267, 433.

Bai, T., Kiplinger, A. L., and Dennis, B. R. 1983 (in preparation).

Bai, T., and Orwig, L. E. 1983 (in preparation).

Bai, T., and Ramaty, R. 1976, Solar Phys., 49, 343.

_____. 1979, Ap. J., 227, 1072.

Canfield, R. C., et al. 1980,

Chupp, E. L. 1982, in Gamma Ray Transients and Related Astrophysical Phenomena, R. E. Lingenfelter (ed.), (New York: American Inst. of Phys.), p. 409.

_____. 1983, Solar Phys. (in press).

Chupp, E. L., Forrest, D. J., Higbie, P. R., Suri, A. N., Tsai, C., and Dunphy, P. P. 1973, Nature, 241, 333.

Chupp, E. L. et al. 1982, Ap. J. (Letters), 263, L95.

Cliver, E. W., Kahler, S. W., and McIntosh, P. S. 1983, Ap. J., 264, 699.

Datlowe, D. W. 1975, Space Sci. Instr., 1, 389.

_____. 1977, Nuclear Instruments and Methods, 145, 365.

de Jager, C. 1969, in COSPAR Symp. on Solar Flares and Space Sci. Res., C. de Jager and Z. Svestka (ed.), (Amsterdam: North Holand), p. 1.

Dennis, B. R., Frost, K. J., and Orwig, L. E. 1981, Ap. J. (Letters), 244, L167.

Dennis, B. R., et al. 1983, NASA TM 83925.

Forrest, D. J., et al. 1981, in Proc. 17th Intl. Cosmic Ray Conf. (Paris), 10, 5.

Frost, K. J., and Dennis, B. R. 1971, Ap. J., 165, 655.

Gardener, B. M., Forrest, D. J., Zolcinski, M.-C., Chupp, E. L., Rieger, E., Reppin, C., Kanbach, G., and Share, G. 1981, Bull. AAS, 13, 903.

Ginzburg, V. L., and Syrovatskii, S. I. 1964, The Origin of Cosmic Rays (New York: MacMillan).

Hoyng, P., Brown, J. C., and van Beek, H. F. 1976, Solar Phys., 48, 197.

Hoyng, P., et al. 1981, Ap. J. (Letters), 246, L155.

Hudson, H. S. 1978a, Solar Phys., 57, 237.

Hudson, H. S. 1978b, Ap. J., 224, 235.

Hudson, H. S., Bai, T., Gruber, D. E., Matteson, J. L., Nolan, P. L., and Peterson, L. E. 1980, Ap. J. (Letters), 236, L91.

Hudson, H. S., Lin, R. P., Stewart, R. T. 1982, Solar Phys., 75, 245.

Kahler, S. W. 1982a, J. Geophys. Res., 87, 3439.

_____. 1982b, Ap. J., 261, 710.

Kane, S. R., and Anderson, K. A. 1970, Ap. J., 162, 1003.

Kane, S. R., Kai, K., Kosugi, T., Enome, S., Landecker, P. B., McKenzie, D. L. 1983, Ap. J. (in press).

Kiplinger, A. L., Dennis, B. R., Frost, K. J., and Orwig, L. E. 1983, Ap. J. (in press).

Lin, R. P., and Hudson, H. S. 1976, Solar Phys., 50, 153.

Lin, R. P., Schwartz, R. A. Pelling, R. M., and Hurley, C. 1981, Ap. J. (Letters), 251, L109.

Lingenfelter, R. E., and Ramaty, R. 1967, in High Energy Nuclear Reactions in Astrophysics, B. S. P. Shen (ed.), (New York: Benjamin), p. 99.

Maxwell, A., and Dryer, M. 1981, Solar Phys., 73, 313.

Nakajima, H., Kosugi, T., and Kai, K. 1982, preprint.

Orwig, L. E., Frost, K. J., and Dennis, B. R. 1980, Solar Phys., 65, 25.

Pesses, M. E., Klecker, B., Gloeckler, G., and Hovestadt, D. 1981, in Proc. 17th Intl. Cosmic Ray Conf. (Paris), 3, p. 36.

Prince, T. A., Ling, J. C., Mahoney, W. A., Riegler, G. R., and Jacobson, A. S. 1982, Ap. J. (Letters), 255, L81.

Ramaty, R., et al. 1980, in Solar Flares, P. A. Sturrock (ed.), (Boulder: Colorado Associated University Press).

Ramaty, R., Kozlovsky, B., and Lingenfelter, R. E. 1975, Space Sci. Rev., 18, 341.

Ramaty, R., Murphy, R. J., Kozlovsky, B., and Lingenfelter, R. E. 1983, Solar Phys. (in press).

Rieger, E. 1982, in Hinotori Symp. on Solar Flares (Tokyo: Inst. Space Astronautical Sci.), p. 246.

Share, G. H., Nolan, P. L., Forrest, D. J., Chupp, E. L., Rieger, E., Reppin, C., and Kanbach, G. 1982, Bull. AAS, 14, 875.

Solar Geophysical Data, Vols. 432-449 (Washington, DC: U.S. Department of Commerce).

Sturrock, P. A. 1974, in Coronal Disturbances, G. Newkirk (ed), IAU Symp. 57, 437.

Sturrock, P. A. 1980, in Solar Flares, P. A. Sturrock (ed.), (Boulder: Colorado Associated University Press), p. 411.

Svestka, Z. 1976, Solar Flares (Dordrecht: Reidel), Chap. IV.

Tsuneta, S., et al. 1982, in Hinotori Symp. on Solar Flares (Tokyo: Inst. of Space and Astronautical Sci.), p. 130.

Vilmer, N., Kane, S. R., and Trottet, G. 1982, Astron. Ap., 108, 306.

von Rosenvinge, T. T., Ramaty, R., and Reames, D. V. 1981, in Proc. 17th Intl. Cosmic Ray Conf. (Paris), 3, p. 28.

Wild, J. P., Smerd, S. F., and Weiss, A. A. 1963, Ann. Rev. Astron. Astrophys., 1, 291.

Yoshimori, M., Okudaira, K., Hirasima, Y., and Kondo, I., 1983, Solar Phys. (in press).

TABLE 1

SMM γ-Ray Line Flares

Date	Hard X-ray Start Time	D (s)	HXRBS Peak Rate (cts s^{-1})	Hα (1)	Location	Radio Bursts (2) II	Radio Bursts (2) IV	Delay (s)	Hard X-Ray Spectral Index	Peak Flux Density at 9 GHz (sfu)
6/07/80	0312:10	60	39000	SN	N14W70	2	1	-	2.8	500
7/01/80	1626:50	180	27000	SB	S12W38	3	2	1.3	3.1	1200
2/26/81	1424:40	120	23000	SB	S13E53	-	-	0.8	3.2	850
6/21/80	0118:20	60	141000	(1B)	N17W91	2	3	-	2.0	1370
9/07/81	2223:00	40	8500	SB	N10E27	3	-	1.5	3.0	1100
11/06/80	0344:40	>420	155000	2B	S12E72	3	3	2.0	3.2	5000
10/14/81	1705:30	>130	44000	(1B)	S06E90	2	2	3.5	3.1	2700
4/01/81	0134:00	1200	12000	3B	S43W52	3	2	8	3.4	4800
10/07/81	2255:40	>480	34000	(1B)	S13E90	2	-	10	3.1	9500
4/10/81	1646:20	>600	12000	3B	N03W38	3	2	10	3.7	1680
4/27/81	0805:00	1320	56000	(2B)	N16W90	2	2	11	3.4	11000
4/26/81	1144:20	>660	7800	2B	N12W74	-	3	120	3.4	10000

(1) Parentheses indicate limb flares.

(2) Numbers indicate intensity classifications (1: < 50 sfu; 2: ~ 500 sfu; 3: > 500 sfu), and short horizontal bars indicate no report in SGD.

TABLE 2

Flares with No Observable γ-Ray Lines

Date	Hard X-Ray Start Time	D (s)	HXRBS Peak Rate (cts s^{-1})	Hα	Location	Radio Bursts (1) II	Radio Bursts (1) IV	Delay (s)	Hard X-Ray Spectral Index	Peak Flux Density at 9 GHz (sfu)	4-7 MeV Excess
3/29/80	0918:05	15	19000	SN	N09W08	-	-	-	3.5	700	-
4/15/80	1509:10	200	19000	SB	N19E12	-	-	-	4.0	79	-
4/28/80	2039:54	10	11000	-	-	-	-	-	4.5	230	-
5/09/80	0712:00	210	11000	1B	S20W35	-	-	-	4.0	200	-
5/21/80	2055:30	60	14000	2B	S13W15	3	3	1	3.6	1250	-
6/04/80	0654:10	60	35000	SB	S14E59	-	-	-	4.0	700	yes
7/21/80	0255:50	120	12000	SN(2)	S15W60	-	-	2	3.5	950	-
9/04/80	0200:50	60	13000	SN	S06W04	1	2	-	4.5	99	(3)
10/09/80	1123:50	80	27000	1B	S21E53	-	-	-	4.5	1015	(3)
10/14/80	0605:20	480	40000	3B	S09W07	1	1	-	6.2	370	-
11/05/80	2232:40	40	13000	2B	N11E07	-	-	-	4.0	2700	-
11/07/80	0204:20	80	87000	2B	N07W11	-	-	-	4.5	7500	yes
11/12/80	0448:20	200	50000	3B	N10W72	-	-	-	4.5	800	yes
11/15/80	1541:10	480	13000	1B	S12W53	-	-	-	5.3	1400	-

(1) Numbers indicate intensity classifications (1: < 50 sfu; 2: ~ 500 sfu; 3: > 500 sfu), and short horizontal bars indicate no report in SGD.

(2) Late observation at 0307 UT.

(3) Rieger (1982) reported that these flares produced a 4 - 7 MeV excess; however, a more detailed analysis shows otherwise (Chupp and Forrest 1983, private communication).

TABLE 3

Delay of Hard X-Rays

Date	Window Time	Ch. 1-2 (29-58 keV)	Ch. 3-5 (58-134 keV)	Ch.6-8 (134-216 keV)	Ch. 9-11 (216-308 keV)	Ch. 12-15 (308-516 keV)
1981 Feb 26	1424:40 ~1424:54	-	0	0.1	0.9	-
1981 Sep 07	2222:45 ~2224:13	0	0	0.5	1.4	1.5
1980 Nov 06	0344:40 ~0348:55	-	0	0.5	1.2	2.2
1981 Apr 01	0133:40 ~0136:20	-0.8	0	1.8	2.7	5.4
	0144:20 ~0147:40	-	0	0.3	2.6	3.3
1981 Oct 07	2255:00 ~2302:40	-	0	1.0	2.7	4.8
1981 Apr 27	0805:40 ~0819:40	-	0	2.0	4.0	7.0
1981 Apr 26	1145:16 ~1147:14	0	27	65	105	114

FIGURE CAPTIONS

Figure 1 Number of hard X-ray events versus HXRBS peak count rate for the 1980-1981 period. During this period, about 4000 solar hard X-ray events were observed by HXRBS; the ones shown here are intense events. The horizontal axis represents the peak count rate measured in the 30 - 500 keV range by HXRBS. From the shaded area, which represents the gamma-ray line flares, we can see that the gamma-ray lines flares are very intense hard X-ray flares.

Figure 2 Hard X-ray (135 ~ 218 keV) time profiles of gamma-ray line flares. It appears that each flare has a characteristic duration for individual bursts. The time profiles are arranged from most impulsive to least impuslive. We find that the characteristic duration of spike bursts changes gradually from the first to the last, instead of there being two groups--impulsive and gradual flares. For some flares the decay phase was not observed because of the eclipse.

Figure 3 Hard X-ray time profiles and a spectrum of the 1981 October 7 flare. We note here a couple of points.

First, we find delays of high-energy hard X-rays when we follow the guidance of two vertical lines. Second, we find that the time profile of 30 - 59 keV X-rays is dominated by a slowly varying component, which keeps increasing after the high-energy time profiles reached the maxima. SMM did not observe the decay phase because of the eclipse at 2302 UT.

Figure 4 Hard X-ray spectra of the 1981 October 7 flare, taken in the interval 2301:28 ~ 2302:15 UT. Notice the low-energy component showing up as excesses over the power-law component. This low-energy component is slowly varying, as seen in Figure 3.

Figure 5 Hard X-ray time profiles of the first of three bursts of the 1981 February 26 flare. For easy comparison, the time profile of the 58 - 134 keV band (X0.02) is shown by a dashed line together with that of the 216 - 309 keV band. Here, we can visually recognize a short delay of ~ 1 s.

Figure 6 Hard X-ray time profiles of the 1981 April 10 flare. Examples of intermediate delays.

Figure 7 Hard X-ray time profiles of the 1981 April 26 flare. Examples of the longest delays. Sudden drops at 1155 UT are due to the eclipse.

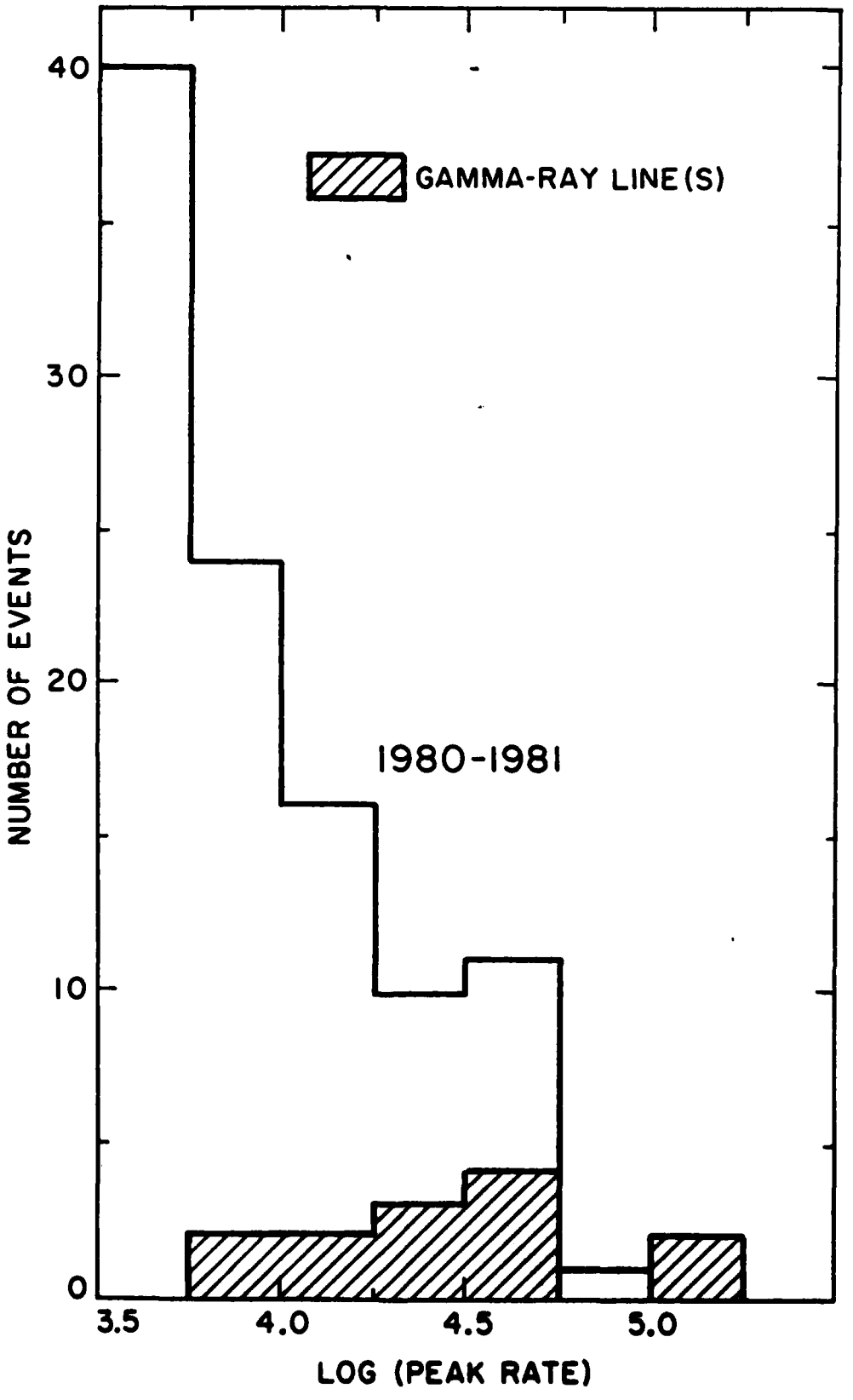
40
30
20
10
0
NUMBER OF EVENTS
GAMMA-RAY LINE(S)
1980-1981
3.5
4.0
4.5
5.0
LOG (PEAK RATE)

Fig. 1

Fig. 1

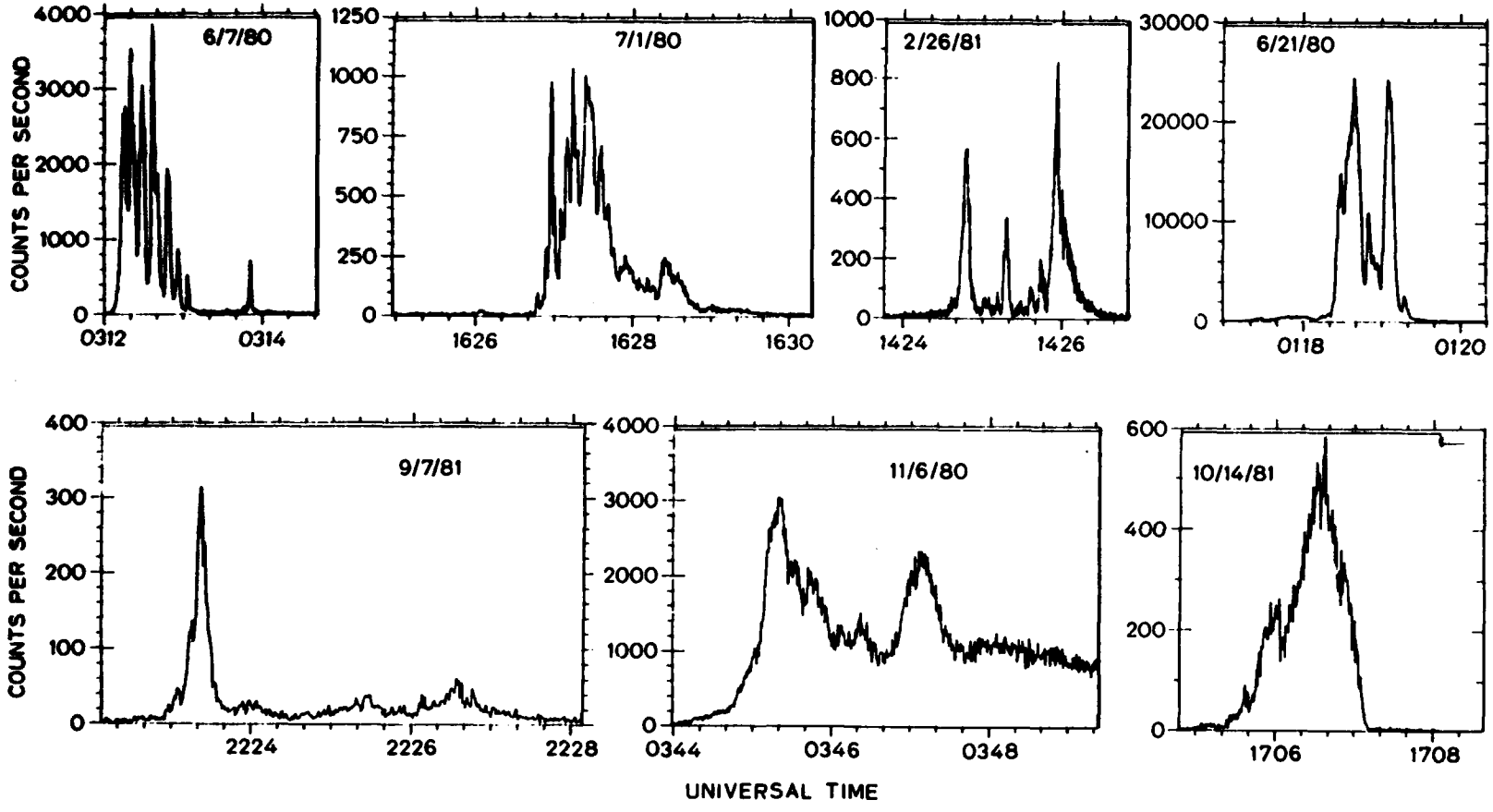
6/7/80
7/1/80
2/26/81
6/21/80
9/7/81
11/6/80
10/14/81
COUNTS PER SECOND
UNIVERSAL TIME
0312
0314
1626
1628
1630
1424
1426
0118
0120
2224
2226
2228
0344
0346
0348
1706
1708

Fig. 2a

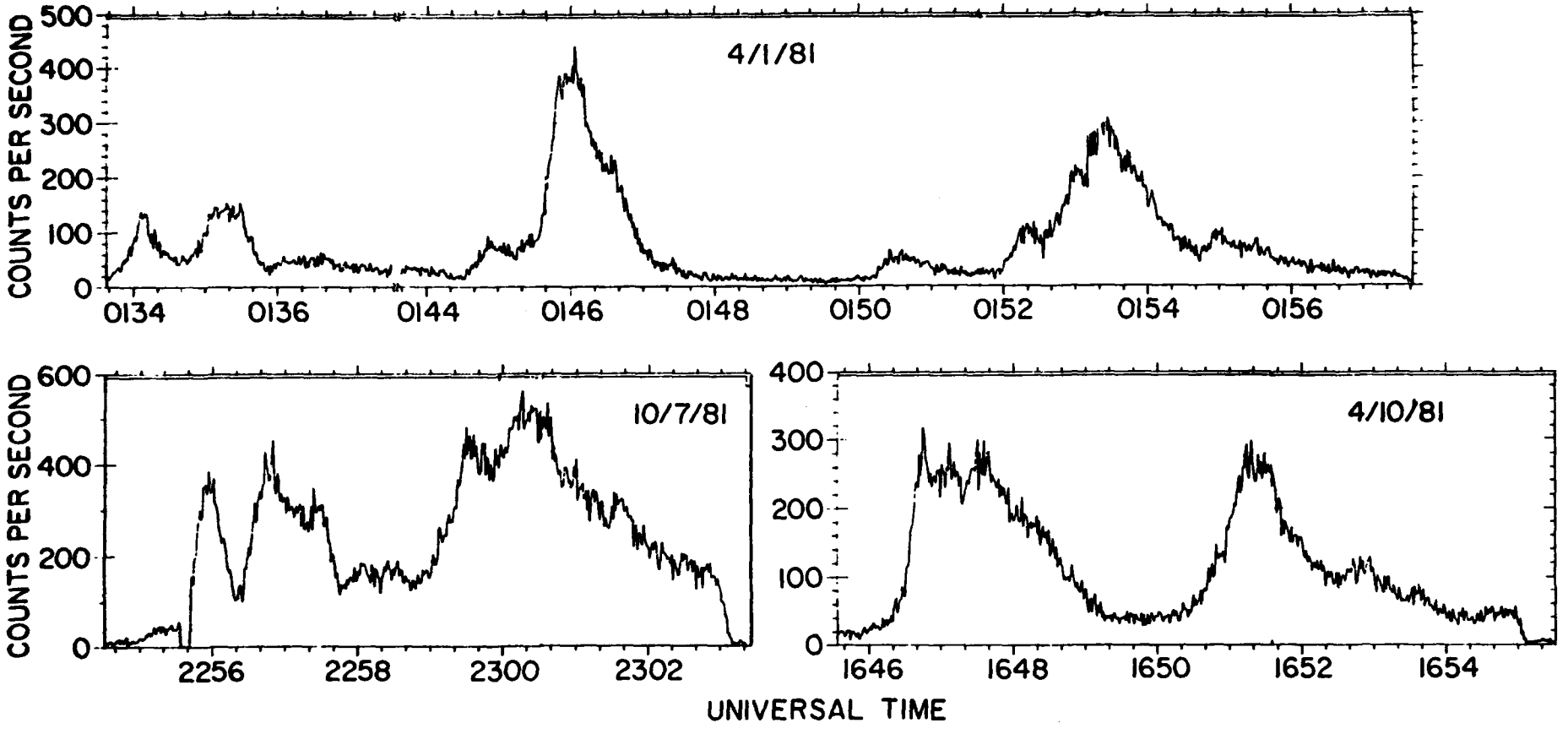
4/1/81
COUNTS PER SECOND
500
400
300
200
100
0
0134
0136
0144
0146
0148
0150
0152
0154
0156
10/7/81
600
400
200
0
2256
2258
2300
2302
4/10/81
400
300
200
100
0
1646
1648
1650
1652
1654
UNIVERSAL TIME

Fig. 2b

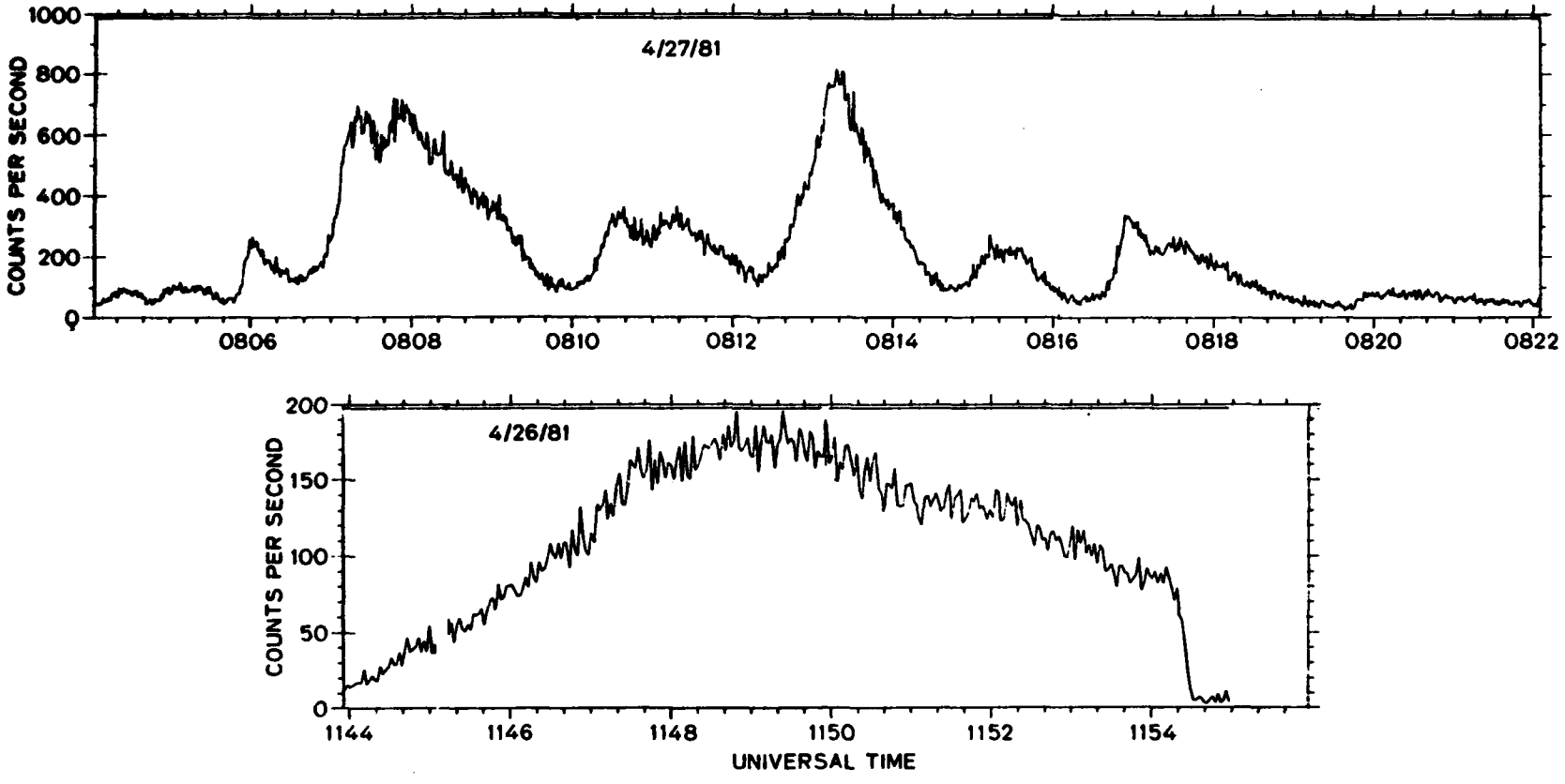
4/27/81
COUNTS PER SECOND
1000
800
600
400
200
0
0806
0808
0810
0812
0814
0816
0818
0820
0822
4/26/81
COUNTS PER SECOND
200
150
100
50
0
1144
1146
1148
1150
1152
1154
UNIVERSAL TIME

Fig. 2c

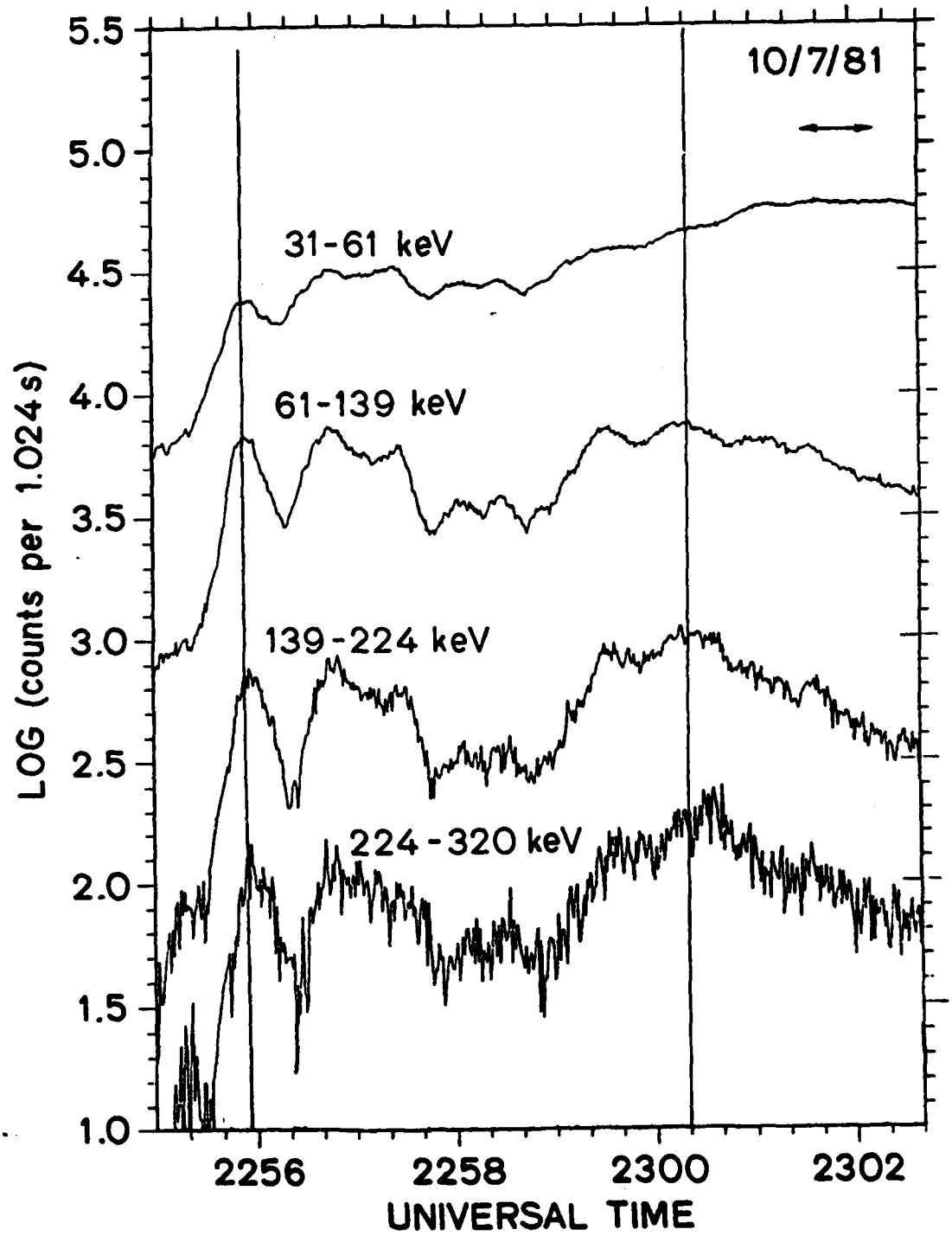
10/7/81
31-61 keV
61-139 keV
139-224 keV
224-320 keV
LOG (counts per 1.024 s)
5.5
5.0
4.5
4.0
3.5
3.0
2.5
2.0
1.5
1.0
2256
2258
2300
2302
UNIVERSAL TIME

Fig. 3

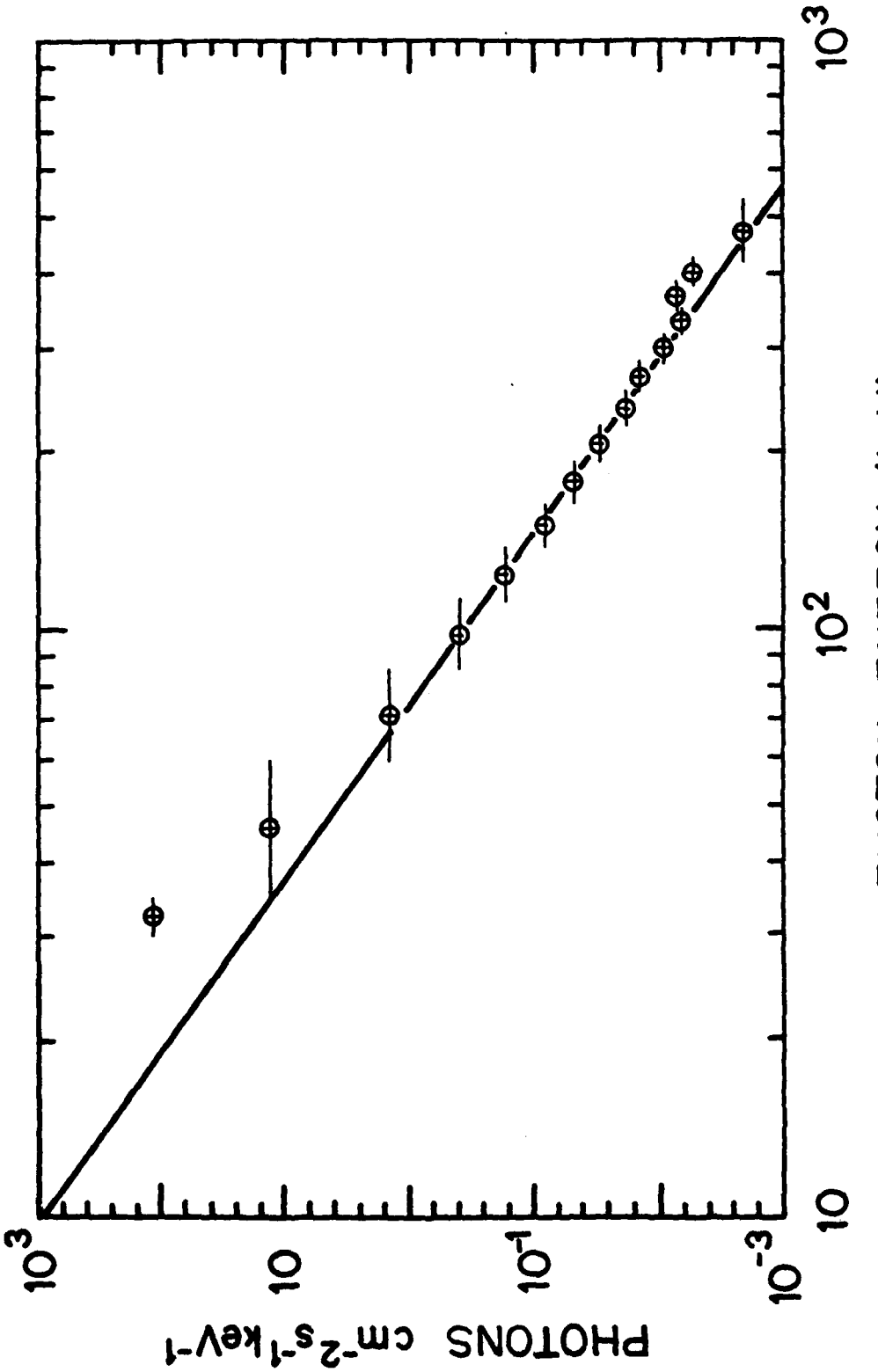
PHOTONS cm⁻²s⁻¹kev⁻¹
10³
10
10⁻¹
10⁻³
10
10²
10³
PHOTON ENERGY (keV)

Fig. 4

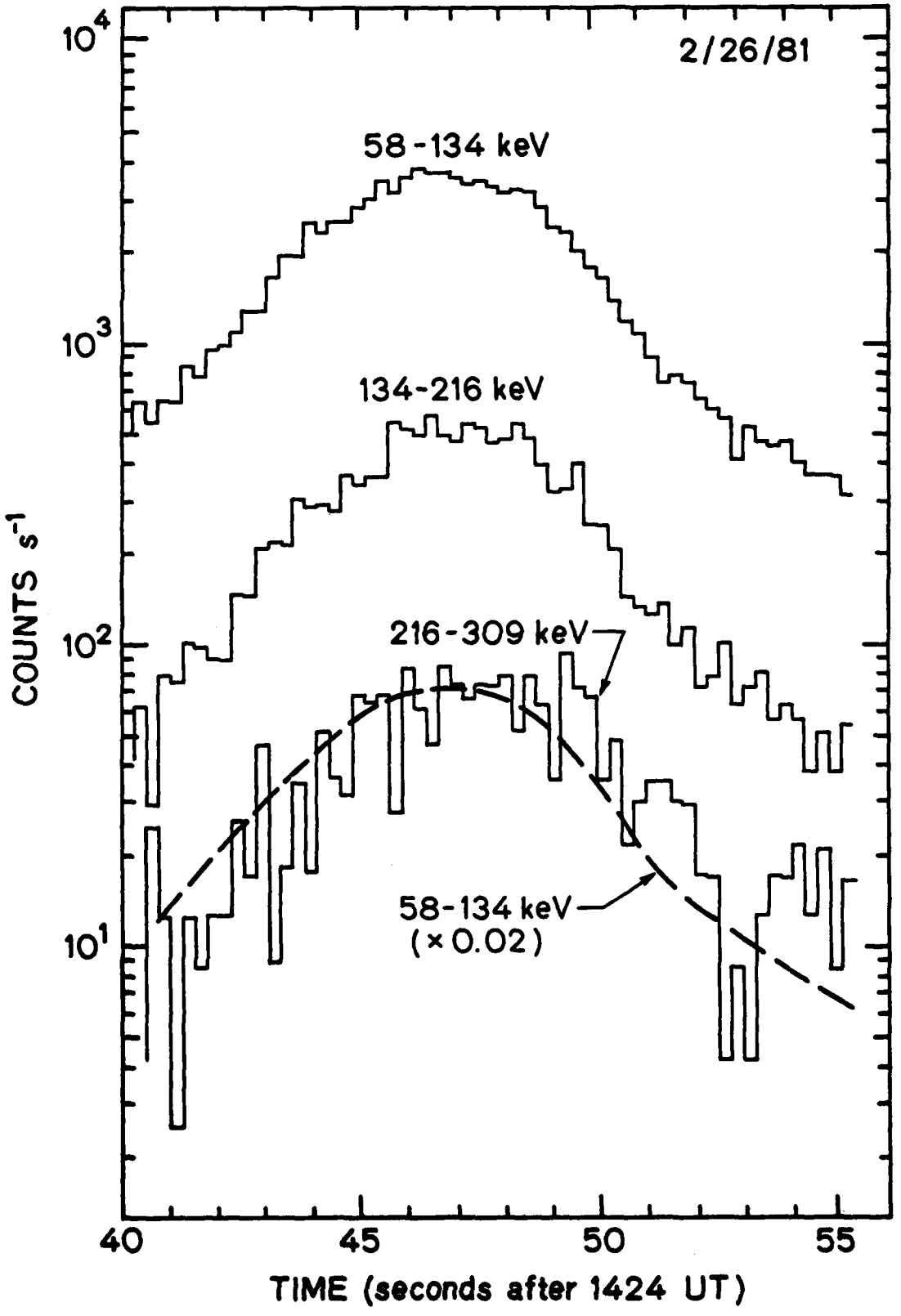
2/26/81
58-134 keV
134-216 keV
216-309 keV
58-134 keV
(×0.02)
COUNTS s⁻¹
10⁴
10³
10²
10¹
40
45
50
55
TIME (seconds after 1424 UT)

Fig. 5

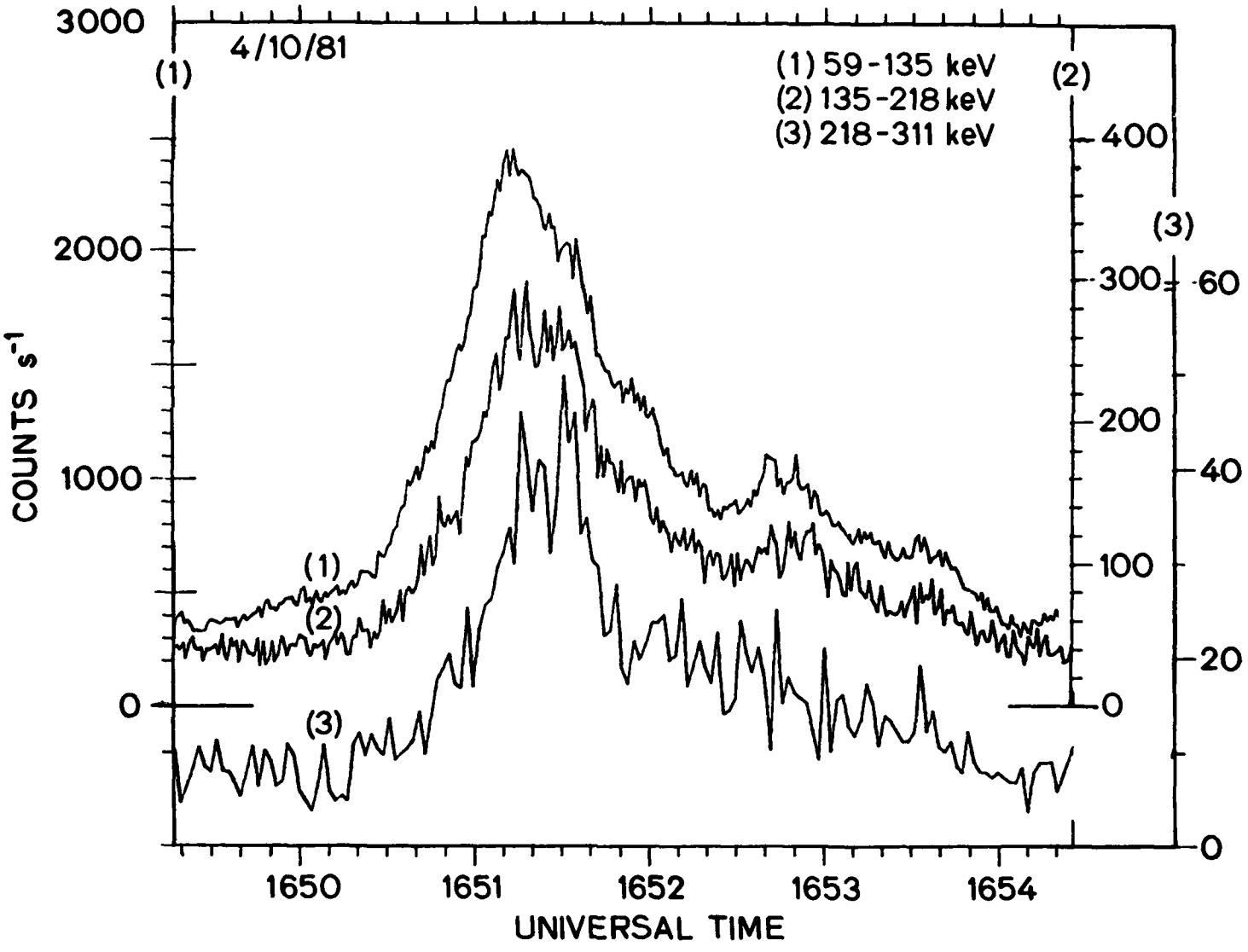
4/10/81
(1) 59-135 keV
(2) 135-218 keV
(3) 218-311 keV
COUNTS s⁻¹
3000
2000
1000
0
(1)
(2)
(3)
400
300
200
100
0
60
40
20
0
1650
1651
1652
1653
1654
UNIVERSAL TIME

Fig. 6

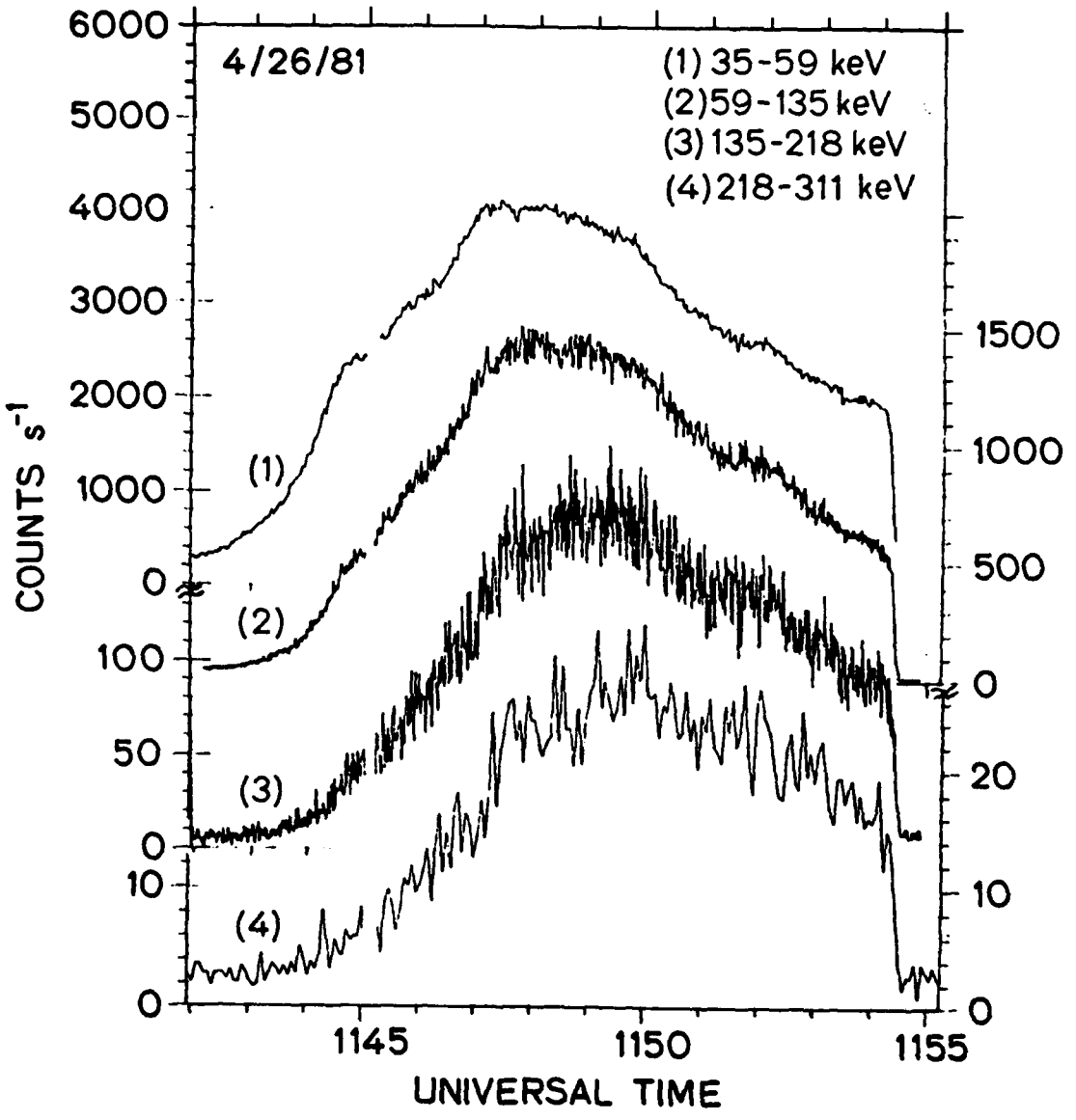
4/26/81
(1) 35-59 keV
(2)59-135 keV
(3) 135-218 keV
(4)218-311 keV
COUNTS s⁻¹
6000
5000
4000
3000
2000
1000
0
100
50
0
10
0
1500
1000
500
0
20
10
0
(1)
(2)
(3)
(4)
1145
1150
1155
UNIVERSAL TIME

Fig. 7